

Electronic Supplementary Information to ‘The role of entropy in nanoparticle agglomeration’

Enno Kätelhön, Stanislav V. Sokolov, Thomas R. Bartlett, and Richard G. Compton*

Oxford Univeristy, Department of Chemistry, Physical and Theoretical Chemistry Laboratory, South Parks
Road, Oxford, OX1 3QZ, United Kingdom

ESI 1 Discussion of systematic errors of the chosen model

Throughout the study, we make the approximation that all agglomeration states are entropically equivalent, i.e. each individual agglomerate features exactly the same entropy independent of the entire system’s entropy. The entropy of a single monomer for instance does not differ from the entropy of an canonical ensemble of the two monomers bound in a dimer and so on. In combination with the more general assumption that all agglomeration states i are energetically equivalent, $E_i = E_0$, we find that the microcanonical partition functions Ω_i of different agglomeration states must be identical:

$$\Omega_i(E_0) = \sum_{r: E_0 < E < E_0 + \delta E} 1 = \text{const.} \quad (\text{ESI 1})$$

where r represents a microstate of the agglomerate.

In an actual particle system, each agglomerate however features additional degrees of freedom that contribute to its entropy and have to be considered in an exact calculation. A monomer, for instance, features three additional rotational degrees of freedom contributing to its microcanonical partition function, while in a larger agglomerate each monomer has three rotational degrees of freedom, various parts of the agglomerate and the entire agglomerate have additional rotational degrees of freedom, and numerous energetically-equivalent microstates may relate to different geometric formations of the monomers in the agglomerate that all contribute to the microcanonical partition function. In environments of low Reynolds numbers, such as the here-investigated agglomeration of nanoparticles, the rotation of agglomerates and the movement of individual monomers within an agglomerate is however significantly hindered by friction and the impact of such additional degrees is therefore lowered.

In a case where all microcanonical partition functions related to each agglomeration state are known, the presented numerical approach can though equally be employed to determine the exact distribution of agglomerate states in the case of maximum entropy. To this end, Equation (1) in the main manuscript is extended by the entropic contributions S_i of individual agglomerates in a specific agglomeration state i :

$$S_i = k_B \ln \Omega_i(E_0) \quad (\text{ESI 2})$$

which leads to a total entropy of the particle population that calculates:

$$\begin{aligned}
S(E_0) &= -k_B N \sum_i x_i \ln x_i + k_B N \sum_i x_i \ln \Omega_i(E_0) \\
&= -k_B N \sum_i x_i \ln \left(\frac{x_i}{\Omega_i(E_0)} \right)
\end{aligned} \tag{ESI 3}$$

The exact distribution of agglomerate states can then be calculated numerically via Lagrange multipliers and the same multi-dimensional Newton Raphson approach specified in the following section ‘Numerical’ in the Electronic Supplementary Information.

ESI 2 Numerical methods

The system of Equations (8) in the main manuscript that was obtained from the transformation of the initially-stated optimisation problem through Lagrange multipliers can be solved numerically via the multi-dimensional Newton-Raphson method. To this end, we redefine the equations in a way that a system of $i_{max} + 1$ equations of the form:

$$f_i(N_1, \dots, N_{i_{max}}, \lambda) = 0 \tag{ESI 4}$$

is resembled, where f is a function $f : \mathbb{R}^{i_{max}+1} \rightarrow \mathbb{R}^{i_{max}+1}$. Using the substitution:

$$\phi = \exp\left(\frac{\lambda}{k_B}\right) \in \mathbb{R}^+ \tag{ESI 5}$$

we eliminate the constant k_B and the exponential function that numerically complicates the calculations though its value is not of physical interest. By this means, we transform (9) in the main manuscript into the desired form by the following definition of f :

$$0 = f_i := \begin{cases} N_{init} - \sum_{k=1}^{k_{max}} i N_j & \text{for } i = 0 \\ \frac{N_i}{\sum_{k=1}^{k_{max}} N_j} - \phi^i & \text{for } i \in [1, i_{max}] \end{cases} \tag{ESI 6}$$

Following the procedure of the multi-dimensional iterative Newton-Raphson method, we start with an initial guess of suitable values for all N_i and λ and approach the exact value during subsequent n_{max} iterations. To this end, the following system of equations is solved in each iteration n :

$$J_{i,j} \cdot \Delta N_j^n = f_i(N_i^n) \tag{ESI 7}$$

and the values N_i are subsequently updated:

$$N_i^{n+1} = N_i^n - \Delta N_i^n \tag{ESI 8}$$

Herein, the matrix J_{ij} represents the Jacobian matrix of f which is defined as:

| Parameter | Explanation | Value |
|-----------|----------------|-------|
| n_{max} | No. iterations | 1000 |
| ϕ^0 | Initial ϕ | 0.2 |
| N_i | Initial N_i | 0.01 |

Table ESI 1: Parameters used in the Newton-Raphson solver when determining the distribution of agglomeration states for the case that agglomerates comprising up to 40 monomers may be present.

$$\begin{aligned}
J &= \begin{pmatrix} J_{0,0} & \cdots & J_{0,j_{max}} \\ & \ddots & \\ \vdots & J_{i,j} & \vdots \\ & \ddots & \\ J_{i_{max},0} & \cdots & J_{i_{max},j_{max}} \end{pmatrix} \\
&= \begin{pmatrix} \partial_\lambda f_0 & \partial_{N_1} f_0 & \cdots & \partial_{N_{i_{max}}} f_0 \\ \vdots & \vdots & \ddots & \vdots \\ \partial_\lambda f_{i_{max}} & \partial_{N_1} f_{i_{max}} & \cdots & \partial_{N_{i_{max}}} f_{i_{max}} \end{pmatrix}
\end{aligned} \tag{ESI 9}$$

On the basis of Equations (ESI 6), the individual elements of J can hence be calculated to:

$$J_{i,j} = \partial_{N_j} f_i = \begin{cases} -j & \text{for } i = 0, j \in [0, j_{max}] \\ -i\phi^{i-1} & \text{for } i \in [1, i_{max}], j = 0 \\ -\frac{N_i}{(\sum_{k=1}^{k_{max}} N_k)^2} & \text{for } i, j \in [1, j_{max}], i \neq j \\ \frac{1}{\sum_{k=1}^{k_{max}} N_k} - \frac{N_i}{(\sum_{k=1}^{k_{max}} N_k)^2} & \text{for } i, j \in [1, j_{max}], i = j \end{cases} \tag{ESI 10}$$

For the purpose of this study, we developed a numerical solver to evaluate the distribution of N_i that is defined through the system of equations (ESI 6) generated within the Newton-Raphson method. During each iteration, the corrections to N_i , ΔN_j^n , are determined via the tridiagonal matrix decomposition of the Jacobian J and subsequent Gaussian elimination. Since the diagonal matrix element $J_{0,0}$ however always equals zero, the two first rows of the system are swapped in order to avoid division through zero in the tridiagonal matrix decomposition. The solver is programmed in *C++* and, for the parameters specified in Table ESI 1, requires a computation time of about one second on a standard personal computer.

ESI 3 Experimental methods

For the comparison between the theoretical model and experimental measurements, we employ data that has been discussed in previous studies by Sokolov¹ *et al.* and Bartlett² *et al.*. This data comprises size distributions of Ag and Bi₂O₃ nanoparticle populations with respect to their monomeric sizes as well as size distributions of agglomerates. While more detailed information on the experimental procedures can be found in the original studies, we below outline the employed approach.

Nanoparticle tracking analysis (NTA) was employed to measure the size distribution of individual

citrate-capped Ag nanoparticles as well as the size distributions of agglomerates of the same particle population as well as of a system of uncapped Bi_2O_3 nanoparticles. To this end, citrate-capped Ag nanoparticles (nanoComposix, San Diego, CA, USA) were sized in deionized water in order to obtain a monomeric particle size distribution. The particles were then transferred into 0.10 M potassium chloride, which facilitates agglomeration by minimising electrostatic forces between adjacent particles as predicted by DLVO theory, and the distribution of now agglomerating particles was measured. In addition to that, we analogously measured the distribution of agglomerating Bi_2O_3 nanoparticles (Nanophase, Romeoville IL, USA) in presence of 0.10 M sodium hydroxide.

NTA measurements were performed using a *NanoSight LM20* microscope (NanoSight, Amesbury, UK) fitted with a 640 nm laser source. The Brownian motion of the particles was recorded for a period of 60 s at a temperature of 25.00 ± 0.05 °C using manual gain and shutter settings. Raw tracking data was obtained and analysed through the *NTA 2.3* software environment, which was used to construct the resultant size distributions. Measurements were repeated three times, while each time a different area of the sample was chosen to achieve a representative view of the sample and to confirm the stability of the distribution on the time scale of the experiments.

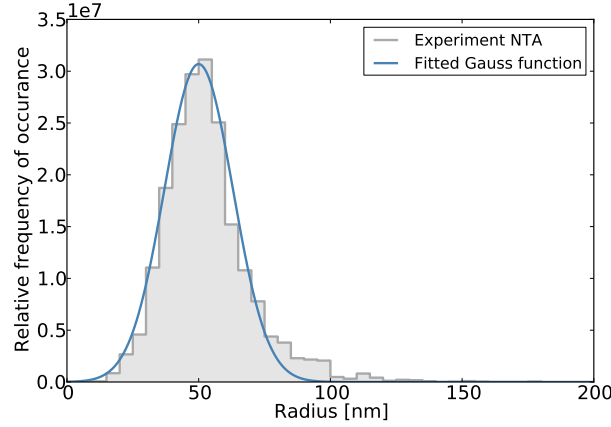
Monomeric distributions of the Bi_2O_3 nanoparticles were gained by nano-impact voltammetry and scanning electron microscopy (SEM) imaging. Nano-impact experiments were conducted in 0.10 M NaOH with a known concentration of Bi_2O_3 nanoparticles added using a *PGSTAT 302N* (Metrohm-Autolab, Netherlands). Reductive potentials from -1.30 V to -1.70 V vs a mercury-mercurous sulfate electrode (MSE) were applied at a 7 μm glass-encapsulated carbon fibre microelectrode (BASi, UK) and current-time transients recorded. The resultant current-spikes attributed to reduction of impacting Bi_2O_3 nanoparticles were analysed using signal counter software³ (Dr. Dario Omanović, Division for Marine and Environmental Research, Ruđer Bošković Institute, Zagreb, Croatia) to obtain the charge passed per spike. The radii of each impacting particle assumes a perfect spherical particle geometries and is discussed in more detail in the original paper². SEM images were taken after impacting Bi_2O_3 nanoparticles on glassy carbon held at a reductive potential of -1.60 V vs MSE with a *Jeol JSM-6500F* field SEM at 5 keV. The resultant images were analysed using the software *image J*. The deposited nanoparticles were found to be near-spherical.

ESI 4 Comparison of theory and experimental data

For the comparison between experimental data on the distribution of agglomerates obtained from NTA via diffusion coefficient measurements and the theoretical prediction, the size distribution of the monomers must additionally be taken into account. Since NTA data solely provides a distribution of the detected object sizes without any direct information on the agglomerate state of the tracked particle or agglomerate while monomer sizes typically vary in accordance with a batch-specific distribution, a continuous distribution rather than sharp lines is usually observed. We therefore first determine the distribution of monomer sizes in the investigated samples and on this basis calculate the distribution expected for the case of maximum entropy by means of Gaussian propagation of uncertainty.

To this end, we fit a Gaussian function to the experimentally found histograms of the size distributions of monomers that were measured via NTA in case of Ag nanoparticles and through nano impacts as well as scanning electron microscopy SEM for Bi_2O_3 . Data is fitted via a least squares approach operating at an accuracy of 1 with respect to the centre of the distribution and the standard deviation. Both the experimental data and the respective fits are depicted in Figure ESI 1. The mean values μ_1 of the monomer radii and the related standard deviation were found to be 50.0 nm and 13.0 nm for μ_1 and σ_1 , respectively, in the case of Ag nanoparticles. We calculate an average of the two

a)



b)

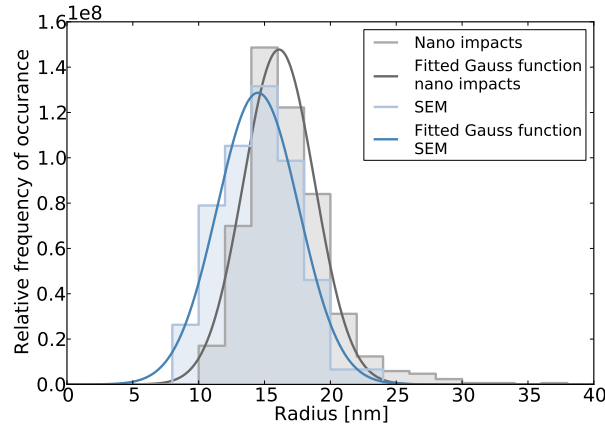


Figure ESI 1: Measured size distribution of monomers in two different nanoparticle systems and corresponding Gaussian fits. a) NTA data¹ of citrate-capped Ag nanoparticles and b) Nano impacts and SEM data² of Bi_2O_3 nanoparticles.

fits related to the Bi_2O_3 measurements and found μ_1 to be 15.3 nm and σ_1 to be 2.9 nm.

Using the approximation that object radii detected in DLS on average simply represent the sum of all radii of the monomers bound in the respective object, we can predict the mean value of the radius of an agglomerate comprising i monomers:

$$\mu_i = i\mu_1 \quad (\text{ESI 11})$$

Herein, we hence use an upper limit for the predicted radii, while actual measurements will lead to lower values. This can be understood by considering the diffusion coefficient of various agglomeration states: Within an agglomerate of a given order, particles may adopt numerous different formations that may each feature varied orientation-dependent diffusion coefficients. Furthermore, agglomerates may alter their formation during the measurement, further complicating the prediction of the NTA result. We therefore choose to model an upper limit by generally assuming all agglomerates to be spherical and featuring the maximum possible radius. If the exact geometrical formation of monomers in each agglomerate was however known alongside the average duration an agglomerate remains in each state, we could carry out an analysis along the lines of Hoffmann⁴ *et al.* and predict the anisotropic translational diffusion coefficients and the NTA distribution on the basis thereof. Via Gaussian propagation

of uncertainty, the standard deviation corresponding to the here-employed approximation calculates to:

$$\sigma_i = \sqrt{i} \sigma_1 \quad (\text{ESI } 12)$$

The overall distribution can then be approximated as a superposition of Gauss functions $f(x, \mu_i, \sigma_i)$ with:

$$f(x, \mu, \sigma) = \frac{1}{\sigma\sqrt{2\pi}} \exp\left(-\frac{(x - \mu)^2}{2\sigma^2}\right) \quad (\text{ESI } 13)$$

weighted by the predicted frequency of occurrence, Equation (12) in the main manuscript, we can predict the continuous distribution $d(x)$ of object sizes expected in a NTA measurement:

$$d(x) = \frac{1}{K} \sum_i \frac{f(x, \mu_i, \sigma_i)}{2^i} \quad (\text{ESI } 14)$$

where K defines the norm:

$$K = \int_0^\infty dx \sum_i \frac{f(x, \mu_i, \sigma_i)}{2^i} \quad (\text{ESI } 15)$$

which is defined in a way that the integral of $d(x)$ equals unity.

References

- [1] Stanislav V Sokolov, Enno Kätelhön, and Richard G Compton. A thermodynamic view of agglomeration. *The Journal of Physical Chemistry C*, 119(44):25093–25099, 2015.
- [2] Thomas R Bartlett, Stanislav V Sokolov, Jennifer Holter, Neil Young, and Richard G Compton. Bi₂O₃ nanoparticle clusters: Reversible agglomeration revealed by imaging and nano-impact experiments. *Chemistry—A European Journal*, 22(22):7408–7414, 2016.
- [3] Joanna Ellison, Kristina Tschulik, Emma JE Stuart, Kerstin Jurkschat, Dario Omanović, Margitta Uhlemann, Alison Crossley, and Richard G Compton. Get more out of your data: A new approach to agglomeration and aggregation studies using nanoparticle impact experiments. *ChemistryOpen*, 2(2):69–75, 2013.
- [4] Martin Hoffmann, Claudia S Wagner, Ludger Harnau, and Alexander Wittemann. 3d brownian diffusion of submicron-sized particle clusters. *ACS Nano*, 3(10):3326–3334, 2009.